

# Morphology in binary blends of poly(vinyl methyl ether) and $\epsilon$ -caprolactone–trimethylene carbonate diblock copolymer

M. C. Luyten, E. J. F. Bögels, G. O. R. Alberda van Ekenstein and G. ten Brinke\*

*Laboratory of Polymer Chemistry and Materials Science Center, University of Groningen, Nijenborgh 4, 9747 AG Groningen, The Netherlands*

and W. Bras

*Netherlands Organisation for Scientific Research (NWO), and Daresbury Laboratory, Warrington WA4 4AD, UK*

and B. E. Komanschek and A. J. Ryan

*Manchester Materials Science Centre, UMIST, Grosvenor Street, Manchester M1 7HS, and Daresbury Laboratory, Warrington WA4 4AD, UK  
(Received 7 November 1995; revised 3 May 1996)*

The morphology of symmetric diblock copolymer of  $\epsilon$ -caprolactone (PCL) and trimethylene carbonate (PTMC), in blends with poly(vinyl methyl ether) (PVME) is investigated with (modulated) differential scanning calorimetry (d.s.c.), time resolved small angle (SAXS) and wide angle (WAXS) X-ray spectroscopy and optical microscopy. In the melt the crystallizable block PCL is immiscible with the amorphous PTMC block. PCL is melt miscible with PVME, whereas PTMC and PVME are immiscible. Despite the much higher molecular weight of PVME, the favourable interaction between PVME and PCL results in a microphase separated morphology with PVME residing inside the PCL domains. In the melt, PVME is for up to 20 wt%, almost homogeneously mixed with PCL. Above 20 wt%, PVME partly segregates inside the PCL domains. In all cases, PCL starts to crystallize from a microphase separated melt. During the crystallization a characteristic small angle scattering peak together with the corresponding wide angle peaks develops. The long period of the crystalline morphology increases as a function of the amount of PVME.  
© 1997 Elsevier Science Ltd. All rights reserved.

(Keywords: block copolymer; blend; crystallization; microphase separation)

## INTRODUCTION

Block copolymers have generated considerable scientific interest due to their remarkable structural and mechanical properties. Commercially important mechanical properties result from microphase separation into microdomains of dissimilar nature, thermoplastic elastomers being a striking example. As a consequence the morphology and phase behaviour of amorphous block copolymers have been studied extensively in recent years. Furthermore, block copolymers play a dominant role in the area of compatibilization and impact modification. Hence, the morphology and phase behaviour in more complicated systems involving additional components such as (a) blends of a block copolymer with a homopolymer, or (b) blends of two non-miscible homopolymers together with a block copolymer with blocks exhibiting selective miscibility with these homopolymers, is also of considerable interest. A wide variety of possible structures arises, depending on thermodynamic as well as kinetic factors. Although the interaction between the different segments, the relative

block length and composition are of major importance, the processing history also plays an important role in attaining the final morphology. Even more complicated structures arise for semi-crystalline block copolymers, which have been studied only recently. Here, the morphology also depends on the outcome of the competition between microphase separation and crystallization.

Microphase separation and the resultant microdomain morphology have been studied extensively for amorphous block copolymers<sup>1</sup>. The order–disorder transition (ODT) is determined by the block incompatibility, usually expressed in terms of the Flory–Huggins  $\chi$ -parameter between the two blocks, the relative length  $f$  and the length of the total polymer ( $N$ ). Ignoring fluctuation corrections, diblock copolymers form a homogeneous phase for  $\chi N < 10.5$ . For  $\chi N$  sufficiently large, the block copolymer will microphase separate into various morphologies, ranging from lamellar to cylindrical to spherical or more complicated, depending on the relative block length  $f$  of the two blocks. Although a lot of work remains to be done here, theoretically these systems are well understood at the mean field level, both in the weak and the strong segregation limit. Currently,

\* To whom correspondence should be addressed

the attention shifts towards the effect of introducing polydispersity in length and chemical composition into the block copolymers, a situation that corresponds more closely to real thermoplastic elastomers<sup>2,3</sup>.

Another area that has attracted quite some interest lately is that of block copolymers consisting of an amorphous block and a crystalline block. Here the possible crystalline domains constitute the physical cross links giving rise to thermoplastic elastomeric behaviour. In these systems, phase separation and microdomain formation can be the result of either block incompatibility or crystallization. Theoretically various models have been developed to describe the thermodynamic equilibrium morphology of semicrystalline block copolymers, in the crystallized state<sup>4-6</sup>. Both the DiMarzio *et al.*<sup>4</sup> theory and the Whitmore and Noolandi approach<sup>5</sup> start from a homogeneous melt from which a lamellar morphology is obtained upon crystallization. Minimization of the free energy results in a morphology of strictly alternating amorphous and crystalline lamellae. The crystalline lamellae consist of regularly folded chains and the thickness of these lamellae is equal to the fold length. In contrast to chain folding in semicrystalline homopolymers, the chain folded morphology is the thermodynamically most favourable situation due to the competition between a reduction in the number of folds per block and the stretching of the amorphous block. However, as in the case of homopolymers where the extended chain crystals correspond to thermodynamic equilibrium, this thermodynamic equilibrium structure is difficult to attain, and various other structures have been reported in the literature.

Ishikawa and coworkers<sup>7,8</sup> studied the morphology of polytetrahydrofuran-block-polyisoprene (PTHF-PIP) diblock copolymer. Solution cast samples consisted of a lamellar structure with domains of the crystallizable PTHF blocks consisting of three layers. The two outer layers correspond to crystalline lamellae, whereas the inner layer consists of amorphous PTHF and small crystallites. They also investigated the influence of the solvent on the final morphology of the pure diblock copolymer obtained by solvent casting<sup>8</sup>. Depending on the preference of the solvent for one of the two blocks, microphase separation occurred before crystallization, or vice versa. The resulting morphologies differed from one another, and the crystallization and the crystallinity were influenced by the path chosen. Vilgis and Halperin<sup>6</sup> considered exactly this kind of situation theoretically. For a selective solvent for the amorphous block, the initial stage corresponds to a crystalline core surrounded by a solvent swollen corona. In this case the characteristic morphologies of amorphous diblock copolymers can be obtained.

Cohen *et al.*<sup>9</sup> studied the morphologies of pure polystyrene-block-hydrogenated polybutadiene (PS-PEB) cast from solution. They also showed that the final morphology was path-dependent. Finally, Ranganathan and coworkers<sup>10-14</sup> investigated extensively the morphology of semicrystalline diblock copolymers. In the case of ethylene-block-ethylene-alt-propylene (PE-PEP), crystallized from the melt, the microphase separation is driven by crystallization and the PE-domains consist of crystalline lamellae together with amorphous material. As expected, a lamellar morphology is found for all relative block lengths  $f$ .

Blends of an amorphous homopolymer hA together with an amorphous diblock copolymer bAB, hA/bAB,

form the next step in complexity. The phase behaviour and the morphologies of these systems have been studied experimentally<sup>15-17</sup> as well as theoretically<sup>18-21</sup>. Depending on the interaction parameter  $\chi_{AB}$  between the A and B segments, the copolymer composition  $f$  and the ratio between the length of the homopolymer  $N_{hA}$  and the length  $N_{bA}$  of the chemically identical block, microphase or macrophase separation will occur. Assuming the incompatibility to be large enough to induce microphase separation, various possibilities arise. For  $N_{hA}N_{bA} > 1$ , the homopolymer cannot enter the A-block copolymer domain, and macrophase separation will occur. For  $N_{hA}/N_{bA} \approx 1$ , the homopolymers will enter the A-block copolymer domain, but segregate in the centre of this domain. Finally, for  $N_{hA}/N_{bA} < 1$ , the homopolymer will behave as a solvent and mix with the A-blocks at the molecular level. In that case the parameter that determines the morphology is the relative amount of homopolymer compared to the amount of block copolymer.

Recently this research has been extended to blends of an amorphous homopolymer hD together with an amorphous block copolymer bAB, where the homopolymer hD has an attractive interaction with one of the blocks (bA), of the block copolymer<sup>22</sup>. Compared to the hA/bAB blends this attraction enhances the miscibility between the homopolymer and the block copolymer, and so for higher  $N_{hD}/N_{bA}$  values the homopolymer may still reside inside the A-block microdomains.

The obvious next step in complexity is formed by blends of an amorphous homopolymer hA together with a semicrystalline block copolymer bAC, where the possible crystallization of the crystallizable block is an additional complicating factor. A symmetric ethylene-propylene diblock copolymer blended with atactic polypropylene, confirmed micro- and macrophase separation in accordance with the model for purely amorphous A/AB blends<sup>23</sup>. In this system microphase separation occurred before crystallization. The crystallization itself was strongly influenced by the different morphologies, induced by the blending with the homopolymer.

In the present paper we present the obvious next step of a blend of a semicrystalline diblock copolymer poly( $\epsilon$ -caprolactone-block-trimethylene carbonate) (PCL-PTMC) with a homopolymer poly(vinyl methyl ether) (PVME) that has a favourable interaction with one of the blocks, PCL in this case. PCL is an easily crystallizable polymer and its crystallization behaviour is well known<sup>24-26</sup>. PVME and PTMC are amorphous polymers with glass transition temperatures ( $T_g$ s) below the crystallization temperature of PCL, so the crystallization of PCL is not hindered by vitrification of either component. PCL and PVME are miscible<sup>27</sup> but PCL and PTMC<sup>28</sup> as well as PVME and PTMC are not. The latter fact is not known in the literature and will be established here by the well known enthalpy relaxation technique<sup>29</sup>. Homopolymer blends of PCL and PVME have been studied before and some of our findings will be compared to it<sup>30</sup>. A symmetric diblock copolymer was synthesized which should, due to the incompatibility between PCL and PTMC, form a lamellar morphology in the melt. Although PVME has a much higher molecular weight than the PCL block, the attractive interaction between PC and PVME is expected to induce miscibility. The phase behaviour and morphology of these blends are studied with optical microscopy.

(modulated) differential scanning calorimetry (d.s.c.) and time resolved small angle (SAXS) and wide angle (WAXS) X-ray spectroscopy.

## EXPERIMENTAL

### Materials

The PCL-PTMC block copolymer used in this study was synthesized by successive anionic polymerization under nitrogen. The  $\epsilon$ -caprolactone monomer was distilled over calcium hydride before use. The trimethylenecarbonate monomer was recrystallized from *o*-xylene and distilled over calcium hydride and copper powder. The toluene was distilled from sodium, and degassed before use. The  $\epsilon$ -caprolactone monomer was polymerized in toluene for 1 h at  $-10^\circ\text{C}$ , with *s*-butyllithium as the initiator. A sample was taken out and terminated in methanol, to determine the molecular weight of the PCL in the diblock. Immediately thereafter the trimethylenecarbonate was added at a temperature of  $+10^\circ\text{C}$ . After 30 min the solution was poured into methanol, terminating the reaction and precipitating the polymer. The polymer was filtered off and dried under vacuum at  $40^\circ\text{C}$ .

$^1\text{H}$  nuclear magnetic resonance (n.m.r.) and  $^{13}\text{C}$  n.m.r. spectra were recorded, on a 300 MHz Varian VXR spectrometer with deuteriochloroform as solvent and TMS as internal standard. The molecular weights of the precursor PC and of the PCL-PTMC were determined with gel permeation chromatography (g.p.c.) and viscosimetry on a Waters 150C ALC/GPC, using chloroform as an eluant and compared with polystyrene standards. The melting temperature ( $T_m$ ) of PCL and the  $T_g$ s of PTMC and PCL were measured with d.s.c. using a Perkin-Elmer DSC-7. The sample was annealed at  $100^\circ\text{C}$  for 5 min. Then the sample was cooled to  $-100^\circ\text{C}$  and kept at this temperature for 5 min. Subsequently the sample was heated at a rate of  $10^\circ\text{C min}^{-1}$  up to  $100^\circ\text{C}$ . To determine the miscibility of PCL and PTMC in the melted state the block copolymer was heated to  $100^\circ\text{C}$  for 5 min, and subsequently quenched in liquid nitrogen. The sample was kept in the d.s.c. apparatus at  $-90^\circ\text{C}$  for 5 min. Subsequently the sample was heated with a heating rate of  $10^\circ\text{C min}^{-1}$ , to determine the  $T_g$ s. The characteristics of the polymer are in Table 1.

### Blends

A 50/50 homopolymer blend of PVME and PTMC was made by solvent casting using chloroform as a mutual solvent. The solvent was evaporated at  $40^\circ\text{C}$  in a vacuum oven. Enthalpy relaxation measurements were carried out on this blend to study the miscibility. The

sample was annealed at  $100^\circ\text{C}$  for 5 min, and subsequently quenched to  $T = -40^\circ\text{C}$ . It was annealed for 90 min at this temperature, and then heated at  $10^\circ\text{C min}^{-1}$ .

Blends of the block copolymer PCL-PTMC and the homopolymer PVME were prepared by solvent casting using chloroform as a mutual solvent. The solvent was evaporated at room temperature during several days.

### Optical microscopy

The crystallization of the PCL block in the blends was investigated with a Zeiss Axiophot microscope equipped with a hot stage. The blends were heated for 10 min at  $100^\circ\text{C}$ , and subsequently isothermally crystallized at the crystallization temperature  $T_c = 46^\circ\text{C}$ . Photographs of the samples between crossed polarizers were taken. The resulting morphologies were studied as a function of blend composition.

### Differential scanning calorimetry

A Perkin-Elmer DSC-7 d.s.c. was used to investigate the blends. The crystallinity  $X_c$  of PCL was measured as a function of composition. Samples were annealed for 5 min at  $100^\circ\text{C}$ , and then quenched to room temperature. After one month they were heated in the d.s.c. at  $10^\circ\text{C min}^{-1}$  up to  $100^\circ\text{C}$ . The melting enthalpy was measured to determine the amount of PCL crystallized. The crystallinity  $X_c$  was determined using:

$$X_c = \frac{\Delta H_{\text{exp}}}{\Delta H_u^0} \quad (1)$$

where  $\Delta H_{\text{exp}}$  is melting enthalpy of the PCL measured, and  $\Delta H_u^0$  is the melting enthalpy of 100% crystalline PCL;  $\Delta H_u^0 = 136.08 \text{ J g}^{-1}$  (ref. 31).

The crystallization of PCL in the blends was determined as a function of composition. The samples were annealed for 5 min at  $100^\circ\text{C}$  and then cooled down at  $10^\circ\text{C min}^{-1}$ . The crystallization exotherm was measured.

To determine miscibility in the melted state the blends were annealed for 5 min at  $100^\circ\text{C}$ , and then quenched in liquid nitrogen. The samples were kept at  $-90^\circ\text{C}$  in the d.s.c. apparatus for 5 min, and subsequently heated at  $10^\circ\text{C min}^{-1}$ .

### Modulated differential scanning calorimetry

Modulated d.s.c. measurements were performed with a DSC 2920 of TA instruments. The samples were annealed for 5 min at  $100^\circ\text{C}$ , quenched in liquid nitrogen, and put in the modulated d.s.c. at  $-90^\circ\text{C}$ . The measurements were taken in a temperature interval from  $-90$  to  $20^\circ\text{C}$ . The underlying heating rate was  $2^\circ\text{C min}^{-1}$ . An oscillation amplitude of  $1^\circ\text{C}$  and an oscillation period of 60 s were used. The  $T_g$ s were determined from the reversing heat flow curve<sup>32</sup>.

### Time resolved SAX/WAXS/d.s.c.

SAXS/WAXS/d.s.c. data were simultaneously collected at beamline 8.2 of the Synchrotron Radiation Source in Daresbury, UK<sup>33,34</sup>. A beam of  $\lambda = 0.152 \text{ nm}$  X-rays was used. The SAXS patterns were collected with a multiwire quadrant detector, located 3.5 m from the sample. The WAXS patterns were collected with a curved knife-edge detector that covers  $120^\circ$  of arc at a radius of 0.3 m. The SAXS patterns were calibrated with a wet rat tail ( $d = 67.0 \text{ nm}$ ), the WAXS patterns were

**Table 1** Characteristics of the polymers used in this study. The  $M_w$  and the  $M_w/M_n$  are determined with g.p.c., the  $T_g$  and the  $T_m$  with d.s.c. PVME was obtained from Janssen Chimica, the PCL-PTMC, the PCL and PTMC were synthesized by the procedure described in this article

Polymer	$M_w$ (g mol <sup>-1</sup> )	$M_w/M_n$	$T_g$ ( $^\circ\text{C}$ )	$T_m$ ( $^\circ\text{C}$ )
Precursor PCL	38000	1.6	-64	+59
PCL-PTMC	72000	1.6	-61 and -15	+59
PVME	114000	2	-25	
PTMC	12000	1.5	-20	

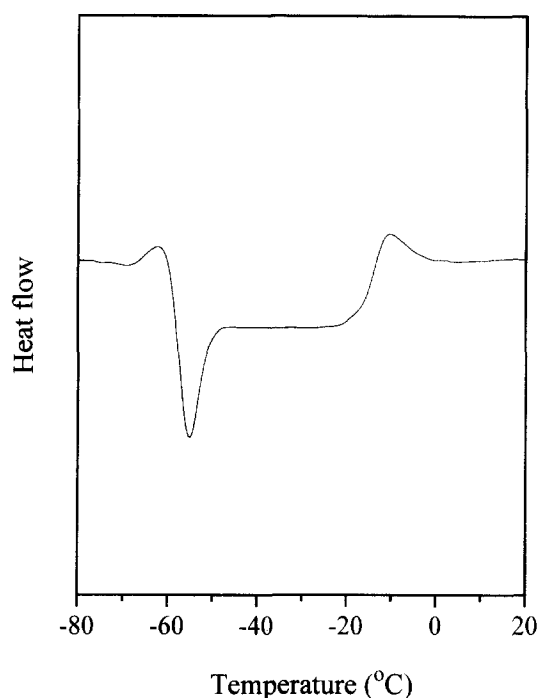


**Figure 1** D.s.c. thermogram of the PCL-PTMC diblock copolymer, quenched in liquid nitrogen. The separated  $T_g$ s of PTMC and PCL are clearly visible at  $-15$  and  $-66^\circ\text{C}$ , respectively, indicating a phase-separated system

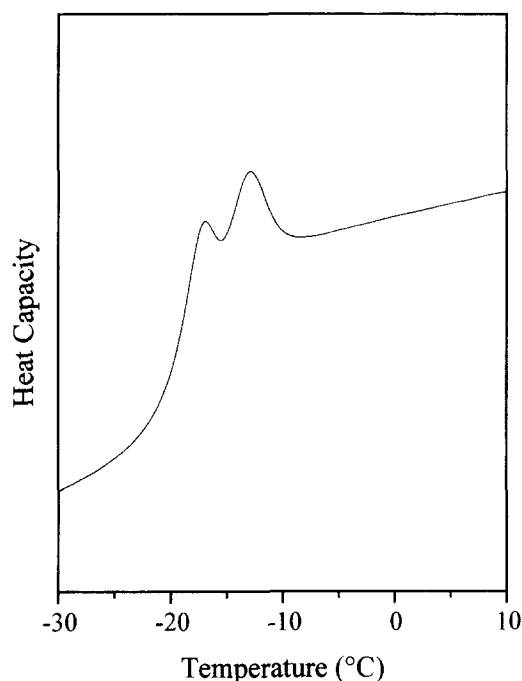


**Figure 2** Enthalpy relaxation thermogram of the hPVME/hPTMC blend. Two different relaxation peaks are clearly visible, indicating phase-separation

calibrated with LDPE ( $d = 0.4166 \text{ nm}$ ). The d.s.c. cell was a modified Linkam THM microscope hot stage. A high-resolution temperature controller was used to control the sample heating. The sample cell consisted of standard aluminium d.s.c. pans (TA instruments) with holes punched in both the pan and the lid and covered with  $0.025 \text{ mm}$  thick mica sheets. A  $1.0 \times 2.5 \text{ mm}^2$  slot in the d.s.c. cell holder and heating block allows the X-ray access to the sample.

Samples of  $1\text{--}2 \text{ nm}$  thickness were prepared. The



**Figure 3** Polarized light microscope photographs of PCL (a), and PCL-PTMC (b), crystallized at  $46^\circ\text{C}$

samples were heated at  $100^\circ\text{C}$  for 5 min, and then cooled down at  $60^\circ\text{C min}^{-1}$  to the crystallization temperature  $T_c = 35^\circ\text{C}$ . The samples were kept at this temperature for about 30 min. Simultaneously SAXS and WAXS patterns were collected in time frames each lasting 100 s. The experimental data were corrected for background scattering, transmission, and detector response. The Lorentz-corrected scattering curve was used to determine the repeat distance (long period) in the sample.

## RESULTS AND DISCUSSION

### Diblock copolymer PCL-PTMC

The characteristics of the synthesized polymers are given in *Table 1*.  $^1\text{H}$  n.m.r. confirmed that the expected polymers PCL and PTMC were formed and that the ratio PCL/PTMC is about 49/51 (monomer/monomer)%<sup>35,36</sup>. Moreover, in the g.p.c. spectrum, only one peak was present. The molecular weight of the PTMC-block is calculated as the difference between the diblock copolymer molecular weight and the precursor PCL molecular weight as evaluated from the g.p.c. data. The ratio PCL/PTMC calculated from the g.p.c. data is 53/47 wt%, which is, to within experimental error, the same as calculated from the n.m.r. spectrum. Therefore the formed copolymer is a diblock copolymer. The relatively high dispersity is due to back-biting reactions<sup>37</sup>.  $^{13}\text{C}$ -n.m.r. confirmed the presence of only two chemical shifts resulting from the TMC-TMC and the  $\epsilon\text{CL}-\epsilon\text{CL}$  sequences.

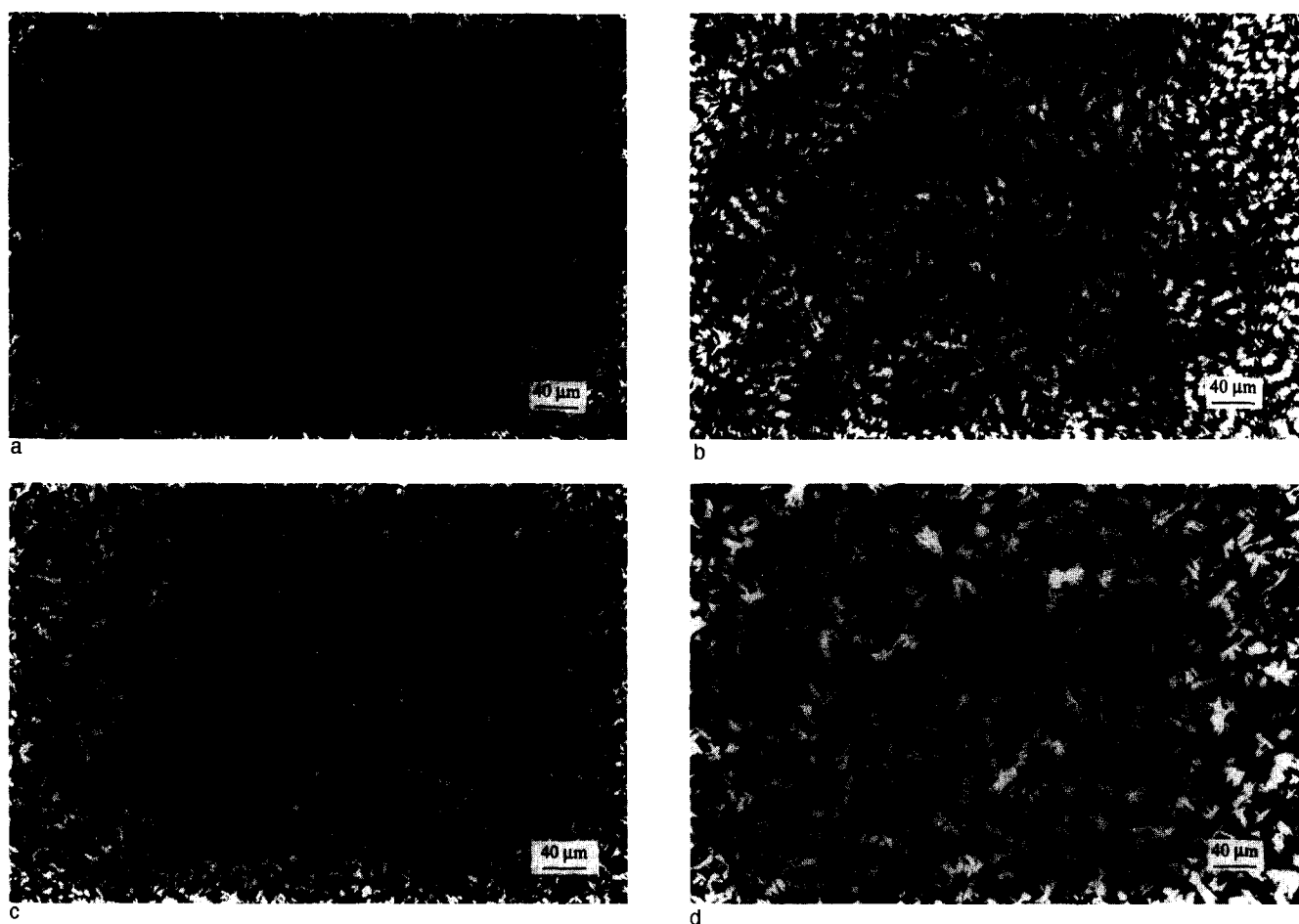


**Figure 4** Polarized light microscope photographs of the blends with PVME crystallized at 46°C. (a) PVME/PCL-PTMC 20/80, (b) PVME/PCL-PTMC 40/60, (c) PVME/PCL-PTMC 60/40, (d) PVME/PCL-PTMC 80/20

Figure 1 shows the d.s.c. thermogram of the diblock copolymer quenched in liquid nitrogen to suppress crystallization of PCL. The  $T_g$  of almost pure PC at  $-66^\circ\text{C}$  is visible. It is immediately followed by a crystallization exotherm and the  $T_g$  of PTMC at  $-15^\circ\text{C}$ . The thermogram clearly confirms that PCL and PTMC are immiscible in the block copolymer melt. Due to the chemical similarity between the two blocks, we were unable to demonstrate the microphase separated structure directly with transmission electron microscopy (TEM). So, although no direct evidence for the morphology is present, the symmetry of the block copolymer strongly suggests that the structure will be a lamellar morphology in the melt<sup>1</sup>, from which the PCL crystallizes upon cooling. In the following discussions we will assume that this is the case.

#### PVME/PTMC miscibility

Before the PVME/PCL-PTMC blends will be discussed in detail, the immiscibility of PVME and PTMC will first be demonstrated by considering a blend of these two homopolymers. The identification of a single composition-dependent  $T_g$  in a mixture of polymers is the most widely applied criterion for determining miscibility, but its applicability is limited by the difference in the  $T_g$ s of the pure components. Typically, when  $T_g$ s are closer than  $10^\circ\text{C}$ , a normal d.s.c. measurement cannot resolve phase differences clearly. As Table 1 demonstrates this is precisely the situation at hand. However, if different phases in the sample are present, they will show a different enthalpy recovery

behaviour after annealing in the glassy state which can be made visible with the familiar enthalpy relaxation measurements<sup>29,38</sup>. In our case already after 90 min annealing of the blend at  $-40^\circ\text{C}$ , already two peaks appear in a subsequent d.s.c. scan, demonstrating that the system contains two different phases. Figure 2 presents the thermogram of this system.

#### Morphology of PVME/PCL-PTMC

**Optical microscopy.** Polarized light microscopy pictures of pure PCL and the pure diblock copolymer PCL-PTMC are shown in Figure 3. The PVME/PCL-PTMC blends at various compositions are shown in Figure 4. All the pictures show a space-filling crystallization; this is even true for the blend with 80% PVME, where only 10% PCL is present. No macrophase separation can be observed in any of these blends so at a macroscopic level, the PVME is in some way mixed with the PCL-PTMC. To demonstrate what happens in the case of macrophase separation between a diblock copolymer and a homopolymer, Figure 5 presents pictures of macrophase-separated blends of PCL-PTMC with a homopolymer PTMC. Given the fact that the molecular weight of the homopolymer ( $M_w = 14\,000$ ) is considerably below that of the PTMC block, macrophase separation was not really anticipated. Since, however, here the objective is merely to show an optical micrograph of a macrophase separated blend involving the PCL-PTMC block copolymer, the underpinning physics will not be considered further. Returning to the

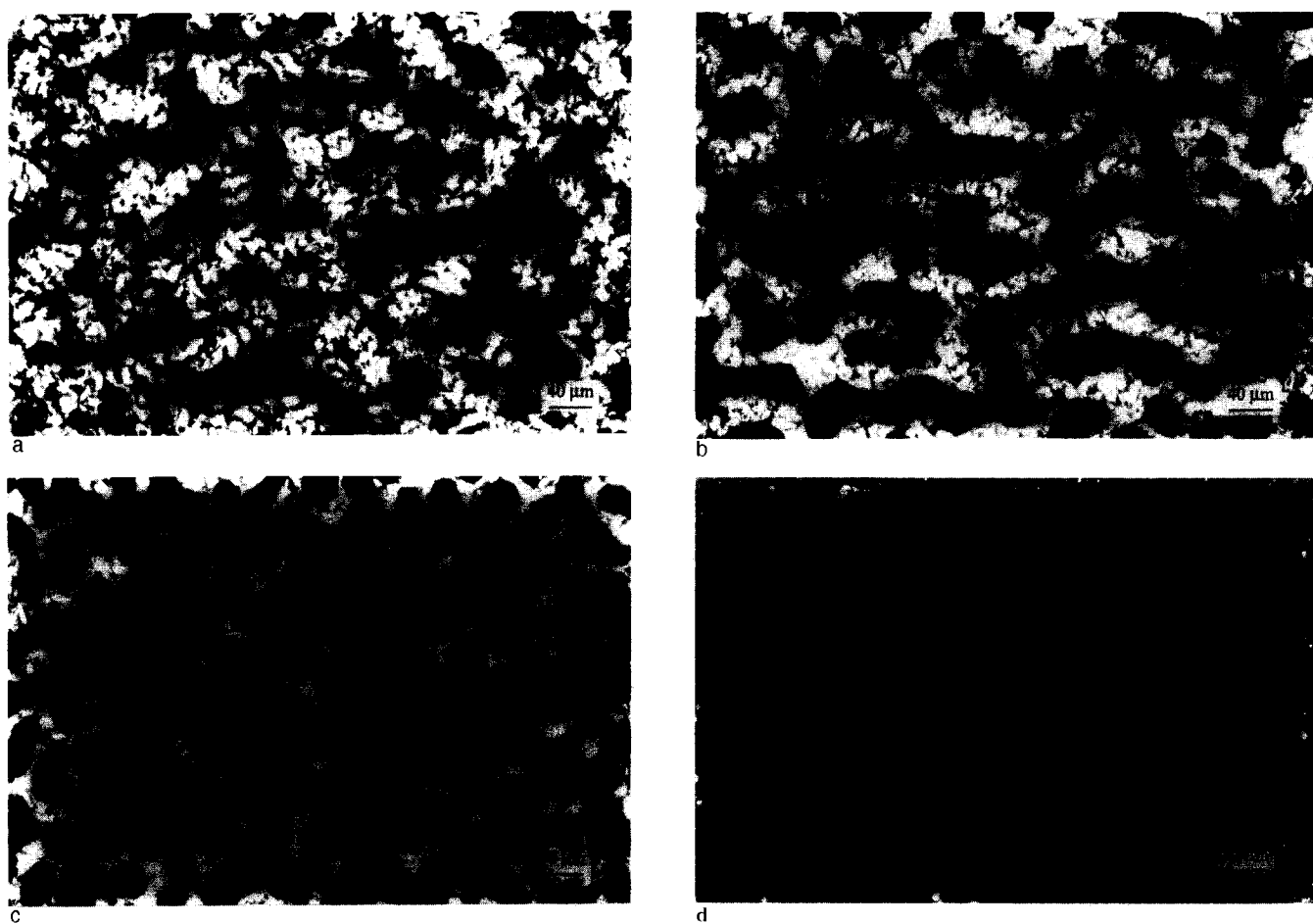


**Figure 5** Polarized light microscope photographs of PTMC blend crystallized at 46 C. (a) PTMC/PCL-PTMC 20/80, (b) PTMC/PCL-PTMC 40/60, (c) PTMC/PCL-PTMC 60/40, (d) PTMC/PCL-PTMC 80/20

PVME/PCL-PTMC blends, *Figure 4* shows a spherulitic morphology for all but the 80/20 composition. In the latter blend, the spherulitic texture is distorted, and a more dendritic-like structure is seen. Here only 10% of PCL is present, and the PCL is so much diluted by the presence of a large amount of amorphous polymer that it can no longer form spherulites but rather forms very open structures.

The spherulites in all these pictures except for pure PCL, show regular concentric rings. These bands are caused by a periodical twisting of the lamellae during crystallization. This phenomenon is known to happen for a few homopolymers, as well as for a blend of two miscible homopolymers, where one of the polymers crystallizes. Ringed spherulites are also reported in a blend of the crystalline homopolymer PCL with the semi-crystalline diblock copolymer PCL-polybutadiene (PCL-PB)<sup>39</sup>. In this case the amorphous block PB caused the PCL lamellae to twist, because it is present interlamellarly, not mixed with the amorphous PCL however. To our knowledge this twisting has never before been reported in pure semi-crystalline diblock copolymers. Extensive discussions about spherulite formation can be found in the literature, but the exact mechanism for the appearance of these bands is still not known. An important observation is that during crystallization the amorphous component remains in between the crystalline lamellae, thus causing the twisting of these lamellae<sup>39</sup>. However, twisting of lamellae has also been reported for a system where the amorphous component resides interfibrillarly<sup>40</sup>. The thickness of the bands decreases with increasing amount of amorphous

polymer. If there is more amorphous material present, the crystalline lamellae twist more.

*Figure 3* shows that ringed spherulites are not present for the pure homopolymer PCL in contrast to the pure copolymer. In the diblock the PCL block is chemically connected to the PTMC block and the PTMC must be located near the PCL crystalline lamellae forcing the PCL lamellae to twist. The blends of the diblock copolymer with PVME also show these ringed spherulites, and with increasing PVME concentration the band thickness decreases. The PVME causes the PCL lamellae to twist more indicating that the PVME is present somewhere near the PCL lamellae. Because PVME is not miscible with PTMC, the PVME is expected to reinforce this twisting having a different spatial orientation with respect to PCL. For the homopolymer blends of PVME and PCL these ringed spherulites are also seen<sup>41</sup>, and there the PVME resides interlamellarly between the PCL lamellae mixed with the amorphous PCL<sup>30</sup>.

*Modulated differential scanning calorimetry.* The crystallinity of PCL in different blends kept at room temperature for 1 month was determined by d.s.c. using equation (1). The results are presented in *Figure 6*. The crystallinity of the block PCL in the pure diblock copolymer is only approximately 50%, and a large amount of amorphous PCL is also present. Since PTMC and PCL are not miscible, the amorphous PCL together with the crystalline PCL forms its own microdomain. In the melt PTMC and PCL have a

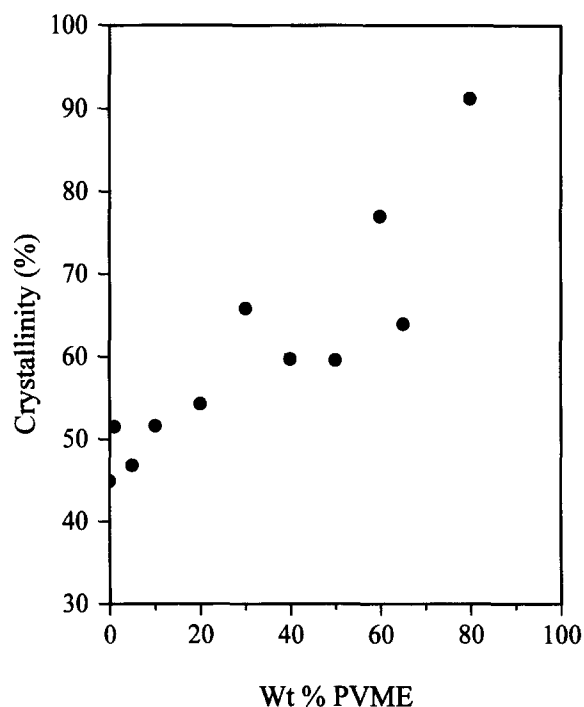


**Figure 6** Crystallinity of PCL as a function of blend composition. The samples were kept at room temperature for 1 month

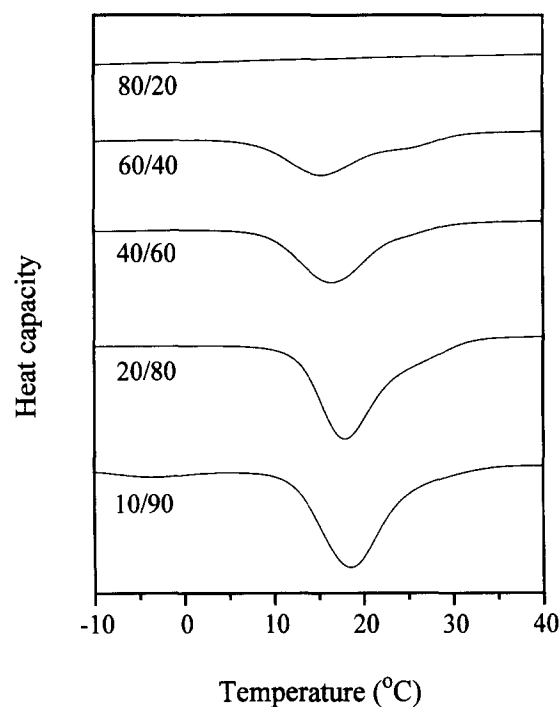


**Figure 8** The crystallization exotherm of PCL in the different blends

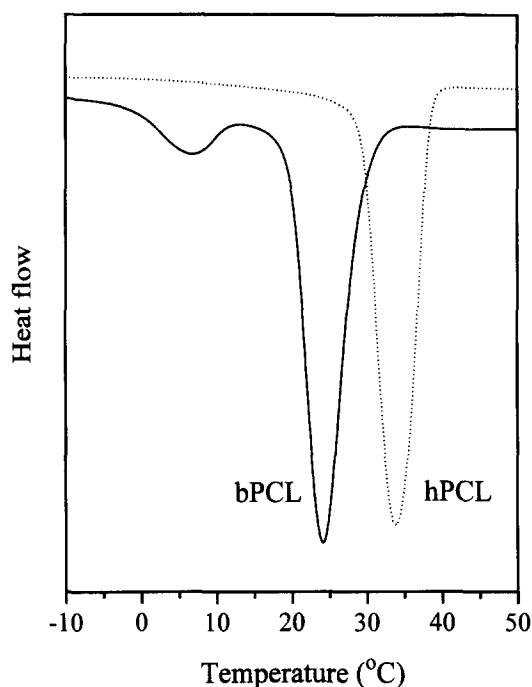


**Figure 7** The crystallization exotherms of the homopolymer PCL and the diblock copolymer PCL, measured with d.s.c.

microphase-separated lamellar morphology and the PCL crystallizes within its own domain. A striking phenomenon is the increase of the crystallinity of PCL with increasing amount of PVME. Apparently the addition of the PVME improves the crystallization of the PCL. The same phenomenon has been reported before for homopolymer blends of PVME and PCL<sup>30</sup>, and the explanation given is that the PVME dilutes the PCL phase approaching gradually the dilute regime from which, at least in solution, single crystals may be obtained. That this behaviour is also present in our

blends, indicates that in the melt of PVME/PCL-PTMC, PVME is mixed at the molecular level with PCL at least to some degree.

The crystallization of PCL during cooling in the d.s.c. with  $10^{\circ}\text{C min}^{-1}$  was also studied. *Figure 7* shows the corresponding characteristic thermograms of pure PCL and pure diblock copolymer. Clearly, both systems behave in a different manner. Whereas the pure PCL shows only one crystallization peak, the copolymer has its main crystallization peak at a lower temperature but more surprisingly also has a second crystallization peak at a much lower temperature. That the main crystallization peak occurs at a lower temperature is not unexpected, since the connection of the PCL to the PTMC block as well as the confinement in a lamellar domain will hamper the crystallization process. The appearance of a second peak indicates the presence of two different crystallization processes. Two crystallization peaks have been reported before for a symmetric diblock copolymer of ethylene and propylene<sup>23</sup>. A similar behaviour was found for PTHF-PI diblock copolymers<sup>7</sup>. In this letter the authors attributed the second peak to crystallization into small crystallites of amorphous PTHF in between the crystalline PTHF lamellae. Apparently, a similar process happens here; subsequently part of the remaining amorphous PCL between the PCL lamellae crystallizes into small crystallites. Blending of the diblock copolymer with PVME changes this behaviour. As demonstrated in *Figure 8*, only the 10/90 blend exhibits two crystallization peaks. Adding more PVME suppresses the low temperature peak, indicating again that PVME resides between the crystalline PCL lamellae molecularly mixed, at least to some degree, with the remaining amorphous PCL, thus preventing its subsequent crystallization.

The results so far demonstrate that the PVME, despite its much larger molecular weight, does not macrophase-separate, and that it resides within the PCL domain. To obtain additional information thermograms of PVME/

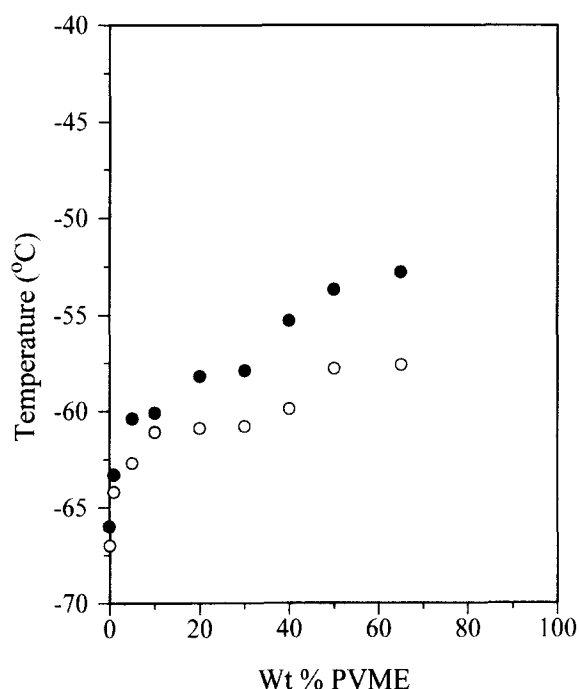


Figure 9 The onset and midpoint  $T_g$  in blends of PVME/PCL-PTMC, as a function of composition.  $\circ$ , onset  $T_g$  PCL;  $\bullet$ , midpoint  $T_g$  PCL

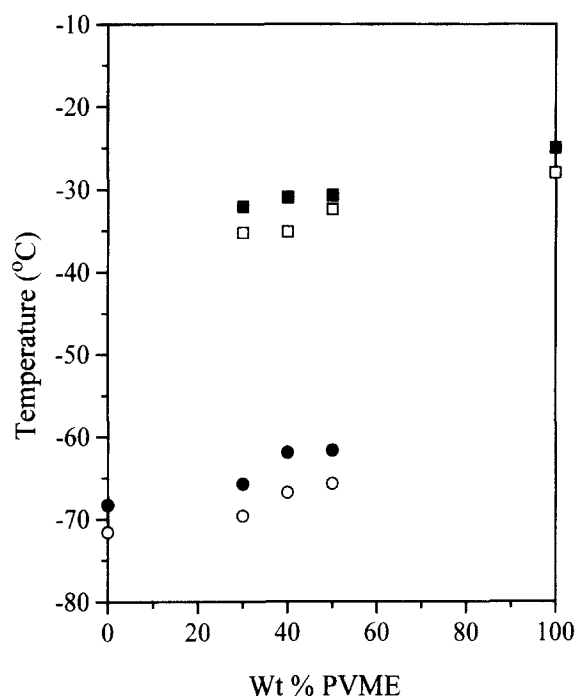


Figure 10 Modulated d.s.c. results. The onset and midpoint  $T_g$ s in blends of PVME/PCL-PTMC, as a function of composition.  $\circ$ , onset  $T_g$  PCL;  $\bullet$ , midpoint  $T_g$  PCL;  $\square$ , onset  $T_g$  PVME;  $\blacksquare$ , midpoint  $T_g$  PVME

PCL-PTMC blends, quenched in liquid nitrogen to prevent crystallization of PCL, were taken. Figure 9 shows the lowest  $T_g$  of the blend as a function of blend composition. With increasing PVME content this  $T_g$ , which is due to the PCL-rich phase, shifts toward higher values. The increase of the  $T_g$ , however, is not as large as expected for a totally miscible system. In fact, Figure 9 suggests that in the melt only a small amount of the PVME (of the order of 10 w/w% PVME/PCL-PTMC) is molecularly mixed with PCL. The additional PVME,

therefore must be segregated as almost pure PVME inside the PCL domains. Hence, a separate  $T_g$  of PVME should be present in blends containing a sufficient amount of PVME. However, once the system passes the  $T_g$  of the PCL-rich phase, PCL starts to crystallize and a possible  $T_g$  is hidden under the crystallization peak and cannot be resolved with conventional d.s.c. Modulated d.s.c. on the other hand offers the possibility of resolving the crystallization exotherm from the glass transition  $C_p$ -jump and a  $T_g$  corresponding to a PVME rich phase, which is presented in Figure 10. Hence, a consistent picture of the morphology of PVME/PCL-PTMC is obtained, which will now be discussed further on the basis of X-ray scattering measurements.

*Small and wide angle X-ray scattering.* SAXS measurements on the pure diblock copolymer at elevated temperatures, i.e. in the melt, did not reveal any features connected to the expected lamellar morphology of the sample. A possibility would be insufficient contrast due to the similarity in chemical structure of both blocks. However, this can easily be ruled out by looking at the scattering of the pure diblock copolymer at room temperature when PCL has crystallized and sufficient contrast between the alternating PTMC and PCL lamellae should be present. But, as will be demonstrated, only one scattering peak corresponding to the long period within the PCL domains due to alternating crystalline and amorphous PCL is present. Probably the long period of the lamellar morphology is too long for the set-up in Daresbury. To demonstrate this, the lower limit for the long period ( $D$ ) will be derived. This can be obtained by considering the weak segregation limit where at the order-disorder transition for a symmetric diblock copolymer ( $D$ ) is related to the radius of gyration ( $R_g$ ) of the symmetric diblock copolymer by<sup>1</sup>:

$$D \cong 3.23 R_g \quad (2)$$

In our case we are dealing with blocks of PCL and PTMC of comparable molecular weight. The radii of gyration of these blocks can be estimated from the general equation:

$$R_g^2 = \frac{1}{6} C_\infty N a^2 \quad (3)$$

Where the characteristic ratio  $C_\infty$  depends on the specific polymer and  $N$  is the number of bonds of average size  $a$ . If experimental data or rotational isomeric state results are unavailable a reasonable estimate can be made using the group method of Van Krevelen<sup>42</sup>. According to this latter procedure and the molecular weights listed in Table 1 we find  $R_g = 7.3$  nm for PCL and  $R_g = 8.3$  nm for PTMC. As a consequence  $D$  should satisfy  $D > 35.7$  nm. In reality, it is much more likely that our system corresponds to the strong segregation limit, in which case, due to considerable chain stretching, the real period will be much longer. The maximum long period that can be seen in the SAXS setup we used is 40 nm, which therefore is too small to observe the long period of our system in the melt state.

The WAXS and SAXS spectra of pure PCL recorded during isothermal crystallization at 35°C are presented in Figure 11. From the Lorentz corrected data the long period is found to be 14.7 nm. The spectra of the pure diblock copolymer PCL-PTMC, presented in Figure 12



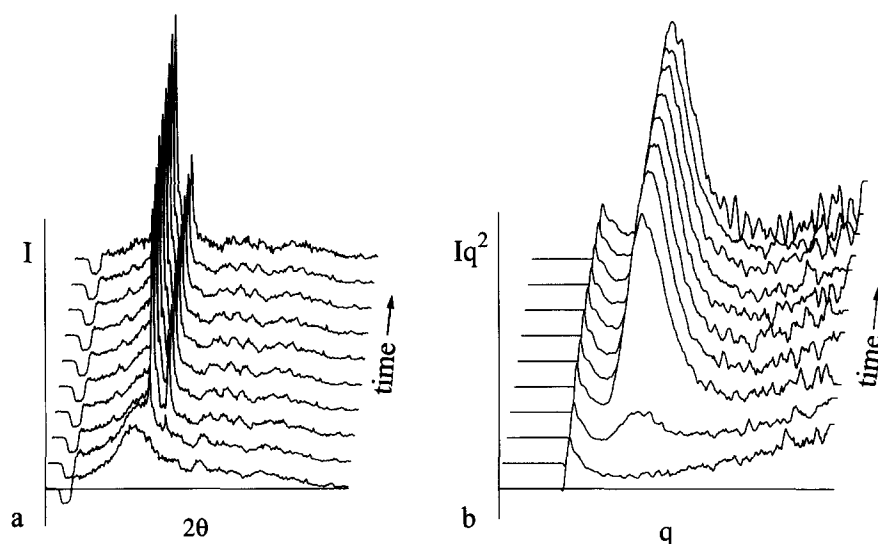


**Figure 11** Time-resolved WAXS (a) and SAXS (b) patterns of pure homopolymer PCL showing the simultaneous appearance of the peaks as a result of isothermal crystallization at 35°C

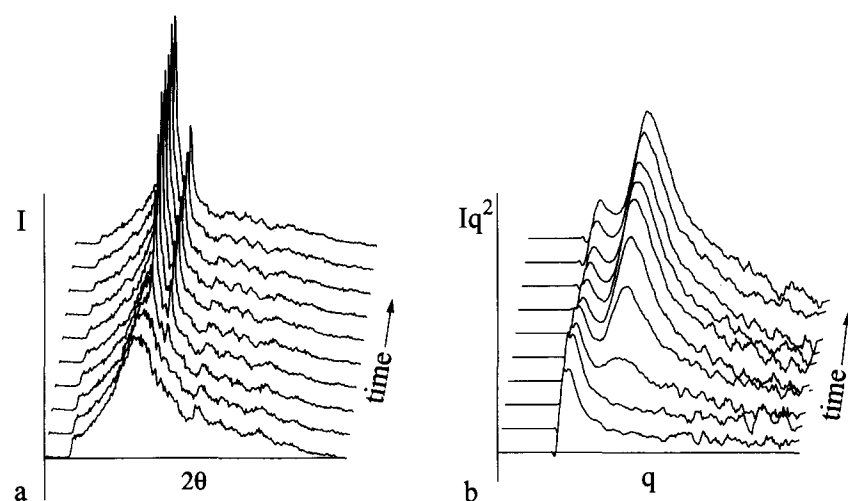


**Figure 12** Time resolved WAXS (a) and SAXS (b) patterns of pure diblock copolymer PCL-PTMC showing the simultaneous appearance of the peaks as a result of isothermal crystallization at 35°C

resemble closely those of pure PCL. The WAXS spectra are identical, whereas the small angle peak is shifted to a smaller angle indicating a slightly larger long period of 16.2 nm. Clearly, this peak also originates from the alternating crystalline and amorphous PCL lamellae distance between the crystalline PCL lamellae.

The angular position of the SAXS peak shifts to smaller angles if PVME is added to the copolymer, and the corresponding long periods are presented in *Figure 13*. The continuous increase in long period ( $L$ ) demonstrates that, as in the case of homopolymer blends of PVME and PCL, PVME resides between the crystalline PCL lamellae. Again, this is in good agreement with the results obtained with the crystallization experiments. According to the dependence of the  $T_g$  on the amount of PVME added, the PVME is present within the PCL domains, but above a given concentration only partially mixed with it, and it partly segregated within the PCL domains.

The crystallinity of the various blends with the same thermal history as those used for SAXS measurements was evaluated from the d.s.c. data. Together with the  $L$

of the SAXS data, the average thickness of the crystalline lamellae and of the amorphous layer was calculated, assuming that all the PVME is situated between the crystalline lamellae of PCL. The wt% of crystalline material  $x_c$  is computed with:

$$x_c = X_c * x_{\text{PCL}} \quad (4)$$

Here  $X_c$  is determined with equation (1) and  $x_{\text{PCL}}$  is the wt% of PCL

$$x_{\text{PCL}} = \frac{w_{\text{PCL}}}{w_{\text{PCL}} + w_{\text{PVME}}} \quad (5)$$

The average thickness of the crystalline lamellae  $l_c$  and the average thickness of the amorphous layer  $l_a$  is computed with

$$l_c = x_c * L \text{ and } l_a = (1 - x_c) * L \quad (6)$$

The results are presented in *Figure 14*. The average thickness of the crystalline lamellae decreases as a function of the amount of PVME added and the increase in long period is entirely due to the increase in amorphous material. This contrasts with our previous

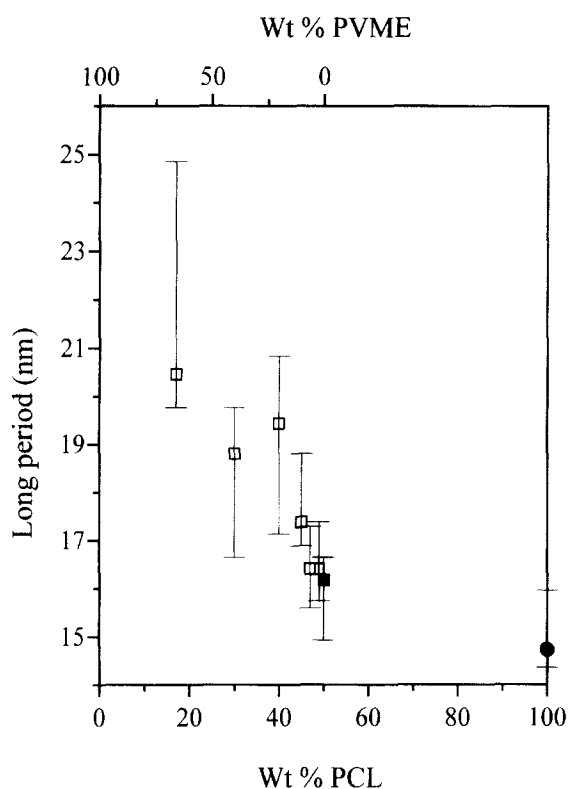


**Figure 13** The long period ( $L$ ) of the crystalline lamellae in the pure homopolymer PCL (●), the pure diblock copolymer PCL (■), and in the blends with PVME (□)

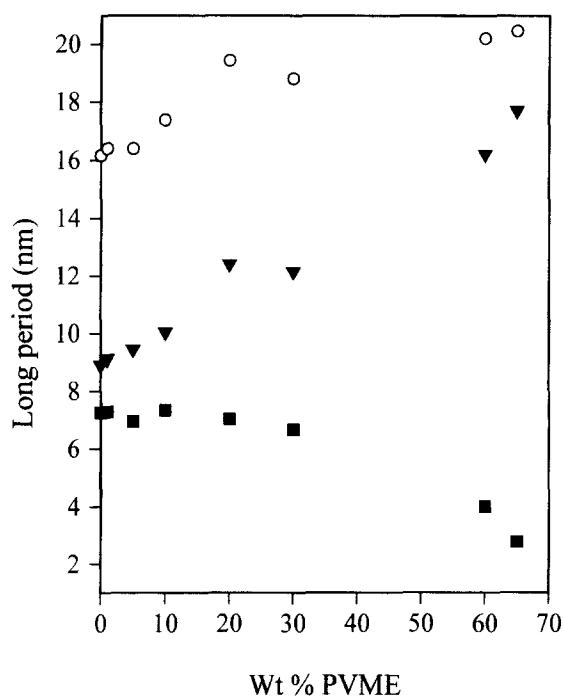


**Figure 14** The thickness of the crystalline lamellae and the amorphous layers as a function of blend composition, computed combining results from d.s.c. and SAXS. Long period,  $L$  (○), amorphous layer,  $l_a$  (▼), crystalline lamellae  $l_c$  (■)

investigation of homopolymer blends of PVME and PCL, where the thickness of the crystalline lamellae remained the same or even slightly increased as a function of the amount of PVME<sup>30</sup>. In that case however the PCL is free to move and crystallizes from a homogeneous melt. The lamellar thickness is completely determined by

the undercooling. In the diblock copolymer PCL together with PVME is confined to the microphase separated lamellae. Moreover, the PCL is covalently linked to PTMC and consequently, the two situations are in some respects totally different.

## SUMMARY

In the melt, blends of homopolymer PVME and diblock copolymer PCL-PTMC have a microphase-separated morphology with the homopolymer PVME residing inside the PCL domains. For moderate concentrations of PVME, PVME is molecularly mixed with PCL. At higher concentrations it segregates partly inside the PCL domains. Upon cooling PCL crystallizes from this pre-existing structure. The long period of the crystalline morphology increases as a function of the amount of PVME and then levels off. This confirms the presence of PVME inside the crystalline PCL lamellae much like the homopolymer blends of PVME and PCL.

## ACKNOWLEDGEMENT

Lizette Oudhuis (University of Groningen) is gratefully acknowledged for her assistance during the measurements at Daresbury Laboratory.

## REFERENCES

- Bates, F. and Fredrickson, G. H. *Annu. Rev. Phys. Chem.* 1990, **41**, 525
- Fredrickson, G. H., Milner, S. T. and Leibler, L. *Macromolecules* 1992, **25**, 6341
- Angerman, H., ten Brinke, G. and Erukhimovich, I. *Macromolecules* 1996, **29**, 3255
- DiMarzio, E. A., Guttman, C. M. and Hoffman, J. D. *Macromolecules* 1980, **13**, 1194
- Whitmore, W. D. and Noolandi, J. *Macromolecules* 1988, **21**, 1482
- Vilgis, T. and Halperin, A. *Macromolecules* 1991, **24**, 2090
- Ishikawa, S., Ishizu, K. and Fukutomi, T. *Polym. Commun.* 1991, **32**, 374
- Ishikawa, S., Sasaki, S. and Fukutomi, T. *J. Appl. Polym. Sci.* 1993, **48**, 509
- Cohen, R. E., Cheng, P. L., Douzinas, K., Kofinas, P. and Berney, C. V. *Macromolecules* 1990, **23**, 324
- Rangajaran, P., Register, R. A. and Fetters, L. A. *Polym. Prep. (ACS)* 1992, **33**, 424
- Rangajaran, P., Register, R. A. and Fetters, L. A. *Polym. Prep. (ACS)* 1993, **34**, 692
- Rangajaran, P., Register, R. A. and Fetters, L. A. *Macromolecules* 1993, **26**, 4640
- Rangajaran, P., Register, R. A., Adamson, D. H., Fetters, L. J., Bras, W., Naylor, S. and Ryan, A. J. *Macromolecules* 1995, **28**, 1422
- Ranfajaran, P., Register, R. A., Fetters, L. J., Bras, W., Naylor, S. and Ryan, A. J. *Macromolecules* 1995, **28**, 4932
- Roe, R. J. and Zin, W. C. *Macromolecules* 1984, **17**, 189
- Winey, K. I., Thomas, E. L. and Fetters, L. J. *J. Chem. Phys.* 1991, **95**, 9367
- Winey, K. I., Thomas, E. L. and Fetters, L. J. *Macromolecules* 1992, **25**, 2645
- Leibler, L. *Macromolecules* 1980, **13**, 1602
- Whitmore, M. D. and Noolandi, J. *Macromolecules* 1985, **18**, 2486
- Semenov, A. N. *Macromolecules* 1993, **26**, 2273
- Matsen, M. W. *Phys. Rev. Lett.* 1995, **74**, 4225
- Löwenhaupt, B., Steurer, A., Hellman, G. P. and Gallot, Y. *Macromolecules* 1994, **27**, 908
- Sakurai, K., MacKnight, W. J., Lohse, D. J., Schultz, D. N. and Sissano, J. A. *Macromolecules* 1994, **27**, 4941
- Phillips, P. J., Rensch, G. J. and Taylor, K. D. *J. Polym. Sci., Part B: Polym. Phys.* 1987, **25**, 1725

- 25 Phillips, P. J. and Rensch, G. J. *J. Polym. Sci., Part B: Polym. Phys.* 1989, **27**, 155
- 26 Hu, H., Dorset, D. L. *Macromolecules* 1990, **23**, 4604
- 27 Watanabe, T., Fujiwara, T., Sumi, Y. and Nishi, T. *Rep. Prog. Polym. Phys.* 1982, **25**, 285
- 28 Albertsson, A. C. and Eklund, M. *J. Polym. Sci., Part A: Polym. Chem.* 1994, **23**, 265
- 29 ten Brinke, G., Oudhuis, A. A. C. M. and Ellis, T. S. *Thermochim. Acta* 1994, **238**, 75
- 30 Oudhuis, A. A. C. M., Thiewes, H. J., van Hutten, P. F. and ten Brinke, G. *Polymer* 1994, **35**, 3936
- 31 Khambatta, F. B., Warner, F., Russell, T. and Stein, R. S. *J. Polym. Sci., Polym Phys. Edn.* 1976, **14**, 1391
- 32 Reading, M., Luget, A. and Wilson, R. *Thermochim. Acta* 1994, **238**, 295
- 33 Bras, W., Derbyshire, G. E., Ryan, A. J., Mant, G. R., Felton, A., Lewis, R. A. Hall, C. J. and Greaves, G. N. *Nucl. Instrum. Methods Phys. Res. Sect. A* 1993, **326**, 587
- 34 Bras, W., Derbyshire, G. E., Devine, Clark, S. M., Cooke, J., Komanschek, B. E. and Ryan, A. J. *J. Appl. Cryst.* 1995, **28**, 26
- 35 Barakat, J., Dubois, Ph., Jérôme, R. and Teyssie, Ph. *Macromol. Commun.* 1991, **24**, 6542
- 36 Albertsson, A. C. and Sjöling, M. *J. Macromol. Sci. A* 1992, **29**, 43
- 37 Hofman, A., Slomkowski, S. and Penczek, S. *Makromol. Chem. Rapid Commun.* 1987, **8**, 387
- 38 Bosma, M., ten Brinke, G. and Ellis, T. S. *Macromolecules* 1988, **21**, 1465
- 39 Nojima, S., Wang, D. and Ashida, T. *Polym. J.* 1991, **23**, 1473
- 40 Defieuw, G., Groeninckx, G. and Reynaers, H. *Polymer* 1989, **30**, 595
- 41 Luyten, M. C., Oudhuis, A. A. C. M., Alberda, G. O. R., ten Brinke, G. to be published
- 42 Van Krevelen, D. W. in 'Properties of Polymers', 3rd Edn, Elsevier, Amsterdam, 1990, p. 250